

The atomic and thermal performance of CuO nanoparticles/paraffin as phase change materials in a circular tube: Molecular dynamics simulation approach

Sabreen Q. Al-Timimy^a, Waqed H. Hassan^{b,c}, Narinderjit Singh Sawaran Singh^d, Ghazi Faisal Naser^{e,f}, Soheil Salahshour^{g,h,i}, S. Mohammad Sajadi^j, Maboud Hekmatifar^{k,*} 

^a University of Misan, College of Engineering, Department of Materials, Engineering, Amarah, Iraq

^b University of Warith Al-Anbiyaa, Kerbala 56001, Iraq

^c Department of Civil Engineering, College of Engineering, University of Kerbala, Kerbala 56001, Iraq

^d Faculty of Data Science and Information Technology, INTI, International University, Persiaran Perdana BBN, Putra Nilai, Nilai 71800, Malaysia

^e Chemical Engineering Department, College of Engineering, Al-Muthanna University, Iraq

^f College of Engineering, Al-Ayen University, Thi-Qar, Iraq

^g Faculty of Engineering and Natural Sciences, Istanbul Okan University, Istanbul, Turkey

^h Faculty of Engineering and Natural Sciences, Bahcesehir University, Istanbul, Turkey

ⁱ Research Center of Applied Mathematics, Khazar University, Baku, Azerbaijan

^j Department of Chemistry, Payam e Noor University, Saqqez Branch, Saqqez, Kurdistan, Iran

^k Fast Computing Center, Shabihzazan Afi Pars, Tehran, Iran

ARTICLE INFO

Keywords:

Phase change material
Atomic and thermal behavior
CuO nanoparticles
Molecular dynamics simulation

ABSTRACT

Background: Using molecular dynamics simulation, this study investigates the effect of CuO nanoparticle addition on the thermodynamic and atomic properties of an octadecane that was being utilized as a phase change material within a circular tube.

Methods: The results indicate that the density (D) was greatest in the vicinity of the tube walls. At its peak, D was 0.0300 atoms per square centimeter. This behavior is due to the increased attractive force that is between the structure's boundaries and its particles. Particle velocity (V) values reached their utmost attainable values in the intermediate regions of the tube, where movement was greatest. At its peak, V was 0.0078 Å/fs. The tube exhibits a maximum temperature (Max T) value of 754.43 K at its midpoint.

Significant Findings: Due to the increased particle motion in the intermediate regions, the investigated structure experienced a greater number of collisions in those areas. After 10 ns, the sample's heat flux, thermal conductivity, and thermal stability converged to values of 3.94 W/m², 1.38 W/mK, and 1821 K, respectively. The structure showed charging and discharging times of 6.41 and 7.15 ns, respectively.

1. Introduction

Thermal energy storage (TES) is an effective way to address differences in energy supply and demand over time, space, and intensity by storing solar energy, recovering industrial waste heat, and using other methods. The installation size, energy storage, D, and technical cost of TES made it advantageous. Compared to sensible heat storage and chemical TES, latent thermal energy storage was more dependable and

constant in terms of T and material [1–3]. Researchers conducted many studies on heat transfer (HT) enhancement of phase change materials (PCMs) composited with nanoparticles (NP) to improve TES efficiency. These materials, which change phases during charging or discharging, include organic, inorganic, and eutectic mixtures, which are used in latent heat storage systems [4,5]. Experimental articles were reviewed in this field, including Pasupathi et al.[6] studied thermo-physical properties of SiO₂/CeO₂ NPs/ paraffin. The results show that by increasing the mass fraction of SiO₂/CeO₂ from 0 % to 2 %, the thermal

Abbreviations: PCM,, Phase change material; TB,, Thermal behavior; MD,, Molecular Dynamics; HF,, Heat flux; TC,, Thermal conductivity; NPs,, Nanoparticles; LJ,, Lennard-Jones; LAMMPS, large-scale atomic/molecular massively parallel simulation.

* Corresponding author.

E-mail address: hekmatifarmabod1361@gmail.com (M. Hekmatifar).

<https://doi.org/10.1016/j.nanoso.2025.101492>

Received 17 June 2024; Received in revised form 22 May 2025; Accepted 26 May 2025

Available online 29 May 2025

2352-507X/© 2025 Elsevier B.V. All rights are reserved, including those for text and data mining, AI training, and similar technologies.

Nomenclature

r_{ij}	The distance between particles (m)
u_i	The potential of a particle (eV)
ϵ_{ij}	Depth of the potential well (kcal/mol)
σ_{ij}	The finite distance in which the potential is zero (Å)
r	The distance of the particles from each other
U_{ij}	The electric potential (eV)
V	The total volume of particles (Å ³)
k_B	Boltzmann constant (1.380649×10^{-23} J·K ⁻¹)
T	The system temperature (K)
J	The heat flux (W/m ²)
m_i	The mass of the particle (g)
a_i	The acceleration of the particle (m·s ⁻²)

conductivity (TC) increased from 0.18 W/m.K to 0.298 W/m.K. Asl-fattahi et al. [7] examined the effect of atomic ratio of Mxene on thermal behavior (TB) of paraffin as PCM. The results show that by adding 0.3 % of Mxene, the TC improved by 16 %. Xu et al. [8] examined the TB of PEG/polyvinyl butyral/graphene nanoplates as PCM composite. At 5 % graphene nanoplates, the PCM composite 3 exhibited a TC of 2.04 W/m.K, which was 8.87 times higher than that of pure PEG. Chen et al. [9] investigated the TB of lauric acid/bentonite/carbon nanofiber composite phase-change materials. The results show that the TC increased from 0.25 W/m.K to 0.52 W/m.K. when the mass fraction of carbon nanofiber was increased from 0 % to 5 %. In the presence of many NPs, an analytical examination of the properties of the molecular system was not feasible. Therefore, studying atomic structures may greatly benefit from the use of the molecular dynamics (MD) simulation method [10,11]. Due to its effectiveness in exploring the mechanisms of atomic interactions, MD simulations were an excellent computational method for studying phase-transition issues at the nanoscale [12,13]. The MD simulation method became more common for atomic structure analysis as a result of advancements in computer programming and simulations [14]. Henda et al. [15] employed MD to simulate perovskite solar cells to suggest a configuration that improves efficiency in challenging environments. The Chebyshev collocation method and a transverse magnetic field were employed by Le et al. [16] to investigate MHD instability in Hartmann flow within porous media. Potential applications in drug delivery and photodynamic therapy were suggested by their findings on nanofluid stability, which are influenced by Hartmann and Reynolds numbers. Functionalized graphene was examined as a nanocarrier for doxorubicin by AlDosari et al. [17] through MD simulations, which demonstrated its efficacy in improving drug transmission to cancer cells. In their investigation of the thermal effects of cross-nanofluids in bio-convection, Aljaloud et al. [18] discovered that the V profile increased with curvature parameters and decreased with the first-order slip parameter, suggesting that the Biot number is a significant factor in the enhanced HT. Banawas et al. [19] conducted a study on the thermal and mechanical properties of reinforced calcium phosphate cement (CPC) using MD simulations. Their findings indicated that the ultimate strength and Young's modulus reduced as the initial temperature rose from 300 K to 400 K, while the inter-atomic distance reduced and the absorption forces among cement particles were strengthened as the initial pressure was increased. Tafrihi et al. [20] emphasized the significance of PCMs in thermal energy storage and transfer, demonstrating that MD simulations effectively addressed thermo-physical challenges and enhanced TC at the nanoscale through molecular orientation. Tafrihi et al. [21] investigated pure tetracosane paraffin and its compounds with graphene and carbon nanotubes. They found that both additives enhanced TC, but they also diminished molecular mobility and thermal capacity. In their investigation of surfactants (SDBS, SDS, Triton X-100) in water/ethylene glycol-graphene nanofluids, Hassanloo et al.

[22] discovered that 0.036 wt% surfactants significantly improved thermophysical properties by increasing TC by 84 % and enhancing viscosity up to 79.36 % with higher SDS levels. Hassanloo et al. [23] developed a technique for stabilizing graphene nanofluids using magnetic NPs and electrohydrodynamic forces, thereby enhancing stability without encountering thermal resistance issues. The settling rates were improved as the graphene concentration increased, with optimal stabilization occurring at an electric field of 0.05 V/Å. Li et al. [24] used MD simulation to investigate the thermal properties of n-octadecane/copper nanofluids as a PCM. The results show that the fluid's thermal properties were improved by the inclusion of copper NPs. Yu et al. [25] utilized MD to study the phase change in NaCl/SiO₂. The simulation results indicated that incorporating SiO₂ NPs resulted in enhanced thermal properties of the PCM, including charging and discharging times, the most significant improvement in TB was observed by adding 2–4 % NPs to the initial structure. Quan et al. [26] studied the TB of ethylene glycol/SiO₂ plates with MD simulation. The greatest D and V were 0.0628 atom/Å³ and 1.851 Å/fs, respectively, according to the data. After 10 ns, TC and heat flux (HF) were 0.85 W/m.K and 8790.83 W/m², respectively. Zhao et al. [10] studied the TB of silica-paraffin utilizing MD simulation. The results show that TC was 0.268 W/m.K. Singh et al. [27] studied the effects of Al₂O₃, MgO, and SiO₂ NPs on the TB of PCM. The results show that the inclusion of these NPs significantly increased charging and discharging rates, but reduced TES capacity. Zhao et al. [28] investigated the effect of adding CuO nanoparticle on thermal properties of paraffin. According to the data, the TC values for paraffin and CuO/paraffin were 0.172 W/m.K and 0.152 W/m.K, respectively. TC increased as the proportion of CuO increased from 0 % to 20 %. Although there were numerous studies that investigated the improvement of thermal properties in PCMs through the incorporation of NPs, this work specifically examined the addition of CuO NPs in octadecane through MD simulation. It built upon and expanded upon these investigations. This research endeavored to offer innovative insights into the optimization of TB and energy storage capabilities of PCM nanocomposites by conducting a systematic evaluation of key parameters, including Max T, D, V, T coefficient, and heat flux. The objective of this research was to enhance comprehension of NP-enhanced PCMs, thereby facilitating the advancement of thermal energy storage systems that are more efficient.

2. MD simulation details

First, a tube with carbon particles was modelled in the simulation box with $50 \times 100 \times 100$ Å³ dimensions. Next, the octadecane as PCMs, water molecules, and CuO NPs with a 1 % atomic ratio were modelled using Avogadro software [29] and packed using Packmol software [30]. In a designed atom-based system, H₂O molecules number set to 200, and the number of PCM molecules is set to 40. Water molecules were modeled by the TIP3P model. A schematic of the structure under study is shown in Fig. 1. A tube model was used to explore this subject. Octadecane was the HT fluid, while PCM was the PCM. Initially, Avogadro software was used to simulate the examined nanostructures. Water molecules were modeled by the TIP3P model. An atomic arrangement was characterized by periodic boundary conditions in the z direction and a fixed boundary condition in the x and y-directions. The use of fixed boundaries in the x and y directions enabled more realistic simulations of macroscopic properties, as the finite character of the tube's length and the interactions with the material were essential to the study's objectives. The configuration was therefore more suitable for the investigation of confined PCM systems, where the thermodynamic behavior was substantially influenced by structural constraints, thereby rendering the results more relevant to practical scenarios. The initial T was estimated to be 300 K. In addition, the time phase was 1 fs, and the simulation duration was 10 ns. Once the investigated structure was modeled, the equilibration of the model was examined. During this phase, the NVT ensemble was used. Once equilibrium was achieved, the NVE ensemble was implemented.

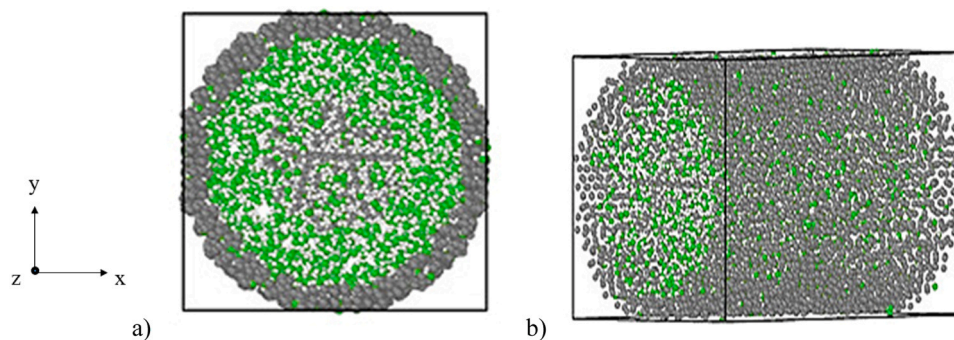


Fig. 1. The arrangement of the structure after observing thermal equilibrium from a) front and b) perspective view at 300 K.

2.1. Equilibration

The TB of simulated samples was thoroughly examined throughout the equilibration stage, leading to the reporting of T and kinetic energy (KE) changes in the atomic samples. In this stage, equilibrium values were computed for samples that did not include NPs. T readings in every sample converged to 300 K as the simulation period increased to 10 ns, suggesting that the atomic structure was in thermodynamic equilibrium. The stability of the structure was validated by the oscillation frequency of structures throughout the simulation box not diverging, which was caused by the T equilibrium in the sample. The stability of atomic samples was suggested by the thermodynamic behavior, which indicated that T fluctuations would eventually become less noticeable. The sample's minimum energy locations caused this process, which guaranteed the system's stability in real-world applications. The results of MD simulations will be trustworthy only if the simulation sample reaches thermodynamic equilibrium. However, the T equilibrium inside the atomic sample indicated that a 10 ns simulation duration was suitable for this study. This part of the study examined the KE changes within the samples. The analysis of KE changes in simulated samples could describe the overall behavior and sustainability of structures. According to the results, KE reached 1.47 kcal/mol. The TB of structure exhibited stability after 10 ns, mirroring the KE behavior observed in the specified sample. KE convergence in atomic structures led to the correlation of oscillatory amplitudes within the structures with particular values as a result of reduced motion of the samples. The number of oscillations decreased due to decreased atom movement inside the simulation box, resulting in a more physically stable structure. This equilibrium was simulated as a result of various components in the structure and the attraction force among NPs. This convergence showed the precise atomic modeling process used, along with the appropriate simulation settings, including the selective force field. These parameters demonstrated that the system reached equilibrium within the specified time frame, further validating the stability of the octadecane shell.

3. Results and discussion

The atomic stability of the sample can be observed via the incorporation of NPs into the phase change structure, as depicted in the atomic image in Fig. 2. In the final phase of the present investigation, the atomic arrangement of PCM in the presence of CuO NPs is illustrated in Fig. 2.

CuO particle's D profile is seen in Fig. 3. As seen in Fig. 3, the highest D was observed close to the channel walls. CuO NPs increased D to a Max of 0.0300 atoms/Å³. The enhanced interaction and attraction force among the particles of the investigated structure and the atomic channel wall was the cause of the highest D in the vicinity of the walls. Confinement effects encouraging aggregation and alignment occurred for NPs as they moved closer to the channel borders, hence increasing the local Den. This effect improved the thermal characteristics of PCM and helped to general system stability and performance. The closeness of

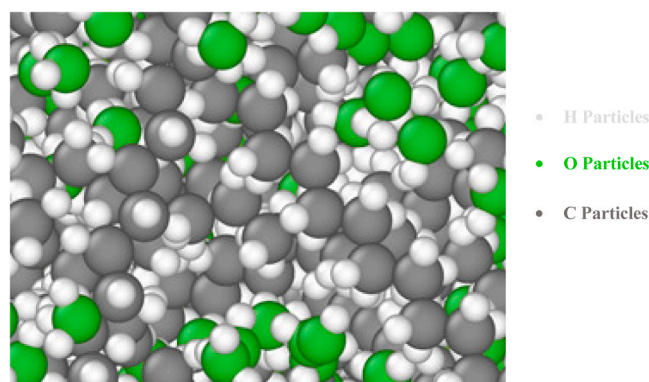


Fig. 2. Atomic arrangement of simulated samples.

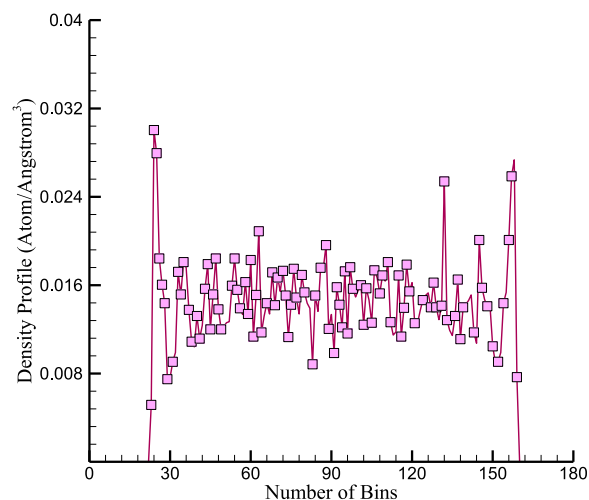


Fig. 3. D profile of octadecane/CuO NPs.

CuO NPs to the walls emphasized the important part of structural design in maximizing thermal management systems by enabling more efficient HT between PCM and the surrounding fluid.

V profile in the simulated atomic sample with PCM and CuO NPs is shown in Fig. 4. Max V value was determined in the central areas of the atomic channel based on Fig. 4. When CuO NPs were present, the highest V value was equivalent to 0.0078 Å/fs. The simulated structure's particle movement increased in the middle sections of the channel because there was a reduction in the attraction force and an increase in the distance among the particles. The increased inter-particle distance in the middle sections of the channel resulted in less hindrance to the particle flow, facilitating enhanced kinetic activity. The incorporation of CuO

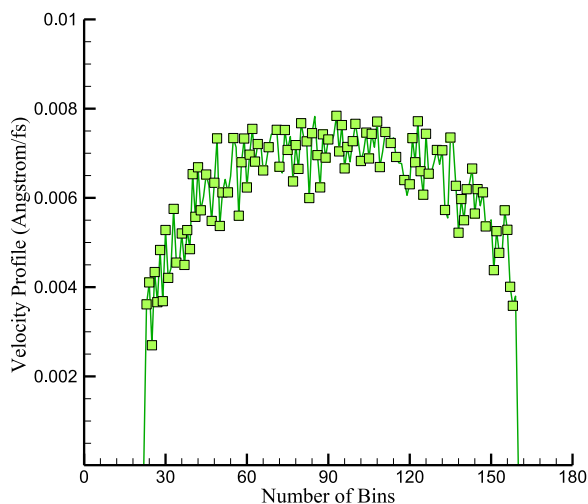


Fig. 4. V profile of octadecane/CuO NPs.

NPs significantly enhanced particle mobility and thermal dynamics within the system by influencing the thermal gradient and HT properties of PCM.

The T profile of the simulated atomic sample in the presence of CuO NPs is depicted in Fig. 5. The results indicate that the highest T was found in the intermediate sections of the atomic channel. When CuO NPs were present, the highest T recorded was 754.43 K. As indicated by the findings presented in the preceding sections, particle collisions increased as V in the intermediate regions of the atomic channel increased. Elevated movement, fluctuations, and particle collisions resulted in a greater number of thermal shocks, which increased the overall temperature of the structure. Though the system was first equilibrated around 300 K, the rise to 754.43 K suggested thermal effects from intensified particle interactions and collisions under CuO NPs. In the intermediate areas, increasing particle collision frequency causes more kinetic energy and corresponding thermal shocks, which explain the higher T. The improved HT dynamics resulting from the presence of CuO NPs, which increased the general thermal responsiveness of PCM, directly cause this phenomenon. The natural result of MD simulation, where particle interactions, thermal fluctuations, and the improved motion of NPs pushed the system towards higher Ts as they collided and exchanged energy, was the rise in T.

In the following, to investigate the TB of the samples as accurately as possible, the HF value and the TC of the final sample were studied. Fig. 6

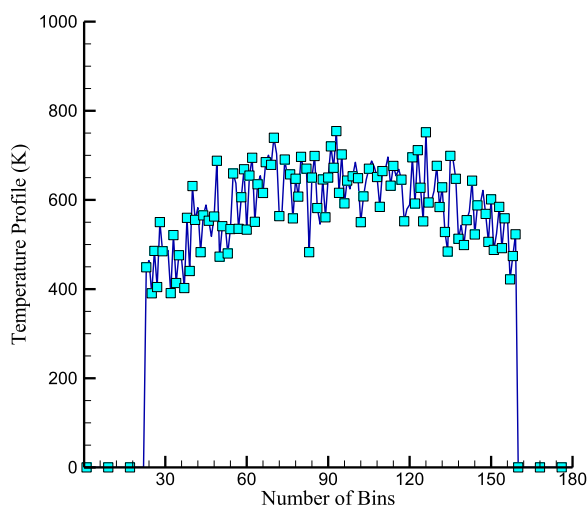


Fig. 5. T profile of octadecane/CuO NPs.

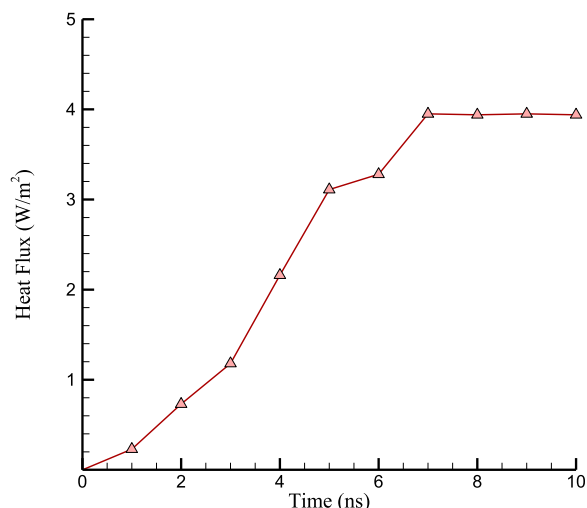


Fig. 6. HF changes by simulation time in the present study.

shows the HF changes over the simulation time in the presence of 1 % CuO NPs. Based on the results presented in this part, the numerical results show the improvement of the TB of CuO NPs. HF was equal to 3.94 W/m² after 10 ns. Therefore, CuO NPs led to the improvement and increase of the TB of the studied structure. NPs functioning as efficient thermal bridges helped to improve energy transmission between the octadecane PCM and the surrounding water molecules. Increased collision frequency and particle kinetic energy brought on by NPs cause more effective thermal exchanges, hence hastening the HT process [31]. Therefore, this improvement guaranteed higher stability during phase transitions, as well as better thermal reaction time of PCM, which was vital for uses in thermal energy storage systems.

TC changes in the sample with time when CuO NPs are present are shown in Fig. 7. Taking into account the direct correlation between HF and TC, TC increased as HF increased and improved. According to the findings in this part, the presence of CuO NPs improved TB. For this sample, the highest TC was 1.38 W/m.K. The dynamic character of molecular interactions and energy transfer within the system accounted for the observed rise in TC during the duration of the simulation, as seen in Figure. Although the system was first equilibrated under the NVT ensemble at 300 K, moving to the NVE ensemble let the particles freely interchange energy and momentum. Accurately recording the real-time variations in TC as the system matures depends on this transition. The

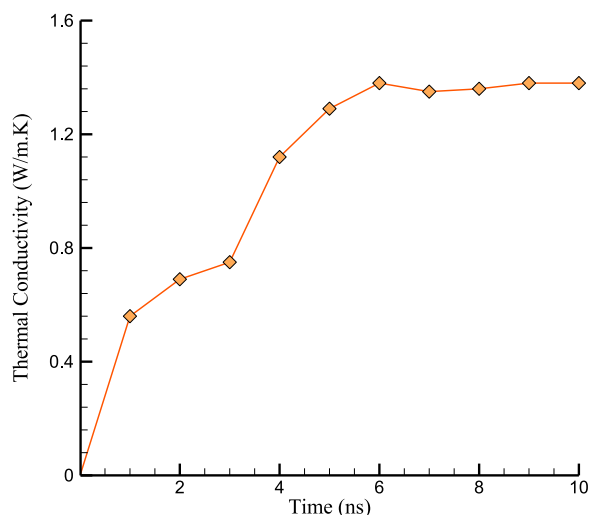


Fig. 7. Changes in the TC by simulation time in the present study.

Table 1
The present simulation details.

Simulation setting	value
Simulation box Dimension	50 × 100 × 100 Å ³
Boundary Condition	ffP
Ensemble	NVT/NVE
Initial T	300 K
Number of H ₂ O Molecules	2000
CuO Nanoparticles Atomic Ratio	1 %
Number of PCM Molecules	40 Molecules
Thermostat	Nose-Hoover
Time step	1 fs
Equilibration process	10 ns
Simulation duration	20 ns

addition of CuO NPs during the simulations caused more particle contact, which in turn raises TC with time. TC naturally increased when particle collisions became more common and energy transfer was enabled by these interactions. The ongoing disturbance of particles, particularly in the presence of NPs, helped to drive this increasing tendency in TC.

This TB resulted from an expansion of the transformation and oscillation ranges of the phase change structure's particles, which increased HT to the target fluid (water molecules). It is expected that this procedure would affect the charging time of the specimen, with a reduction in charging time observed in the presence of NPs and in the final structure. To be more precise, the phase transition process increased when TB was enhanced in the presence of NPs. Thus, the charging period was reduced as the phase transition procedure was completed in a reduced amount of time. The charging time was the duration of time necessary for PCM to absorb heat and transition from a solid to a liquid state [32]. The rate at which the PCM can store heat energy from the surrounding environment was determined by this process, which was essential for thermal energy storage applications. The enhanced TB within PCM was the direct cause of the observed reduction in charging time in the presence of CuO NPs. The incorporation of NPs improved the TC, which in turn facilitated a more efficient HT to the PCM. Consequently, this increase in HT resulted in a more rapid phase transition, which enabled the PCM to achieve its liquid state more quickly. The obtained numerical results for this section are presented in

Appendix A. MD simulation method

Besides, MD simulations can help researchers in obtaining a better understanding of the fundamental principles that govern the behavior of matter at the atomic and molecular levels, with significant implications for various fields, including materials science and biophysics. Newton's second law of motion is expressed as follows:

$$F_i = m_i a_i = -\nabla_i U = -\frac{dU}{dr_i} \quad (\text{a-1})$$

Over the years, this algorithm was extensively studied and optimized, making it a standard tool in the field of computational physics. Using the Verlet algorithm in computer simulations, researchers can gain insights into the behavior of complex systems and develop new materials and technologies with a wide range of applications. This algorithm is expressed as follows [33,34]:

$$r_i(t + dt) = r_i(t) + v_i(t)dt + \left(\frac{F_i(t)}{2m_i}\right)(dt)^2 \quad (\text{a-2})$$

$$v_i\left(t + \frac{dt}{2}\right) = v_i(t) + \frac{dt}{2} \frac{F_i(t)}{m_i} \quad (\text{a-3})$$

Table 2
Numerical results were achieved from the thermal and atomic transformation of the simulated sample for Octadecane/ CuO.

Physical quantity	Max			HF (W/m ²)	TC (W/m.K)	Time (ns)		Thermal stability (K)
	D (atom/Å ³)	V (Å/fs)	T (K)			Charge	Discharge	
Octadecane/ CuO	0.0300	0.0078	754.43	3.94	1.38	6.41	7.15	1821

Table 1. The charge and discharge times for CuO NPs were 6.41 and 15.7 ns, respectively, as shown in **Table 1**.

4. Conclusion

Numerous studies focused on enhancing the HT efficiency of PCMs using NPs, which included organic, inorganic, and eutectic mixtures in latent heat storage systems. This study employed MD simulations to investigate the effects of CuO NP addition on the thermal and atomic properties of octadecane, analyzing key parameters, such as Max T, D, V, HF, and TC. A summary of numerical results follows:

- Max D near the tube walls was recorded at 0.0300 atom/Å³ due to the increased attractive forces between the boundaries and particles.
- Particle V peaked at 0.0078 Å/fs within the central regions of the tube, where movement was most pronounced.
- The highest T observed was 754.43 K at the tube center, correlating with increased particle movement and collision frequency.
- After 10 ns, the HF, TC, and thermal stability stabilized at 3.94 W/m², 1.38 W/m.K, and 1821 K, respectively.
- The structure demonstrated charging and discharging times of 6.41 ns and 7.15 ns.

CRediT authorship contribution statement

Sabreen Q.Al-Timimy, Waqed H. Hassan: Writing – review & editing; Conceptualization, Data curation, Formal analysis; Supervision, Investigation; Writing – original draft; Writing – review and editing. **Narinderjit Singh Sawaran Singh, Ghazi Faisal Naser:** Formal analysis, Data curation, Conceptualization. **Soheil Salahshour; S. MohammadSajadi; Maboud Hekmatifar:** Writing – review & editing; Conceptualization, Data curation, Formal analysis; Supervision, Investigation; Writing – original draft; Writing – review and editing.

Declaration of Competing Interest

The authors declare that they have no known competing financial interests or personal relationships that could have appeared to influence the work reported in this paper.

$$v_i(t+dt) = v_i\left(t + \frac{dt}{2}\right) + \left(\frac{dt}{2} \frac{F_i(t+dt)}{m_i}\right) \quad (\text{a-4})$$

The potential function defines the energy of the system based on the positions of atoms, and its choice greatly affects the accuracy and reliability of simulation results. The potential function of Lennard-Jones was used to simulate the interaction of particles. This function was used for the interactions between two neutral particles or molecules. The typical representation of the Lennard-Jones potential function is expressed as Eq. (a-5) [35, 36]:

$$U_{LJ} = 4\varepsilon_{ij} \left[\left(\frac{\sigma_{ij}}{r}\right)^{12} - \left(\frac{\sigma_{ij}}{r}\right)^6 \right] \quad (\text{a-5})$$

The ε_{ij} and σ_{ij} of each particle in the simulation are reported in Table (a-1) and Eqs. (a-6 and a-7)[37]:

Table a-1
Parameters of the Lennard-Jones potential function for this simulation [38,39]

Particle type	ε_{ij} (kcal/mol)	σ_{ij} (Å)
C	0.105	3.851
H	0.044	2.886
H (H ₂ O)	0.046	0.4
O (H ₂ O)	0.1521	3.1507

$$\varepsilon_{ij} = \sqrt{\varepsilon_i \varepsilon_j} \quad (\text{a-6})$$

$$\sigma_{ij} = \frac{\sigma_i + \sigma_j}{2} \quad (\text{a-7})$$

The equilibrium dynamics method was used to investigate the thermal properties in MD in this research Green-Kubo equation was applied to calculate the TC of modeled structures, as outlined in reference [40].

$$k = \frac{V}{k_B T^2} \int_0^\infty \langle J_x(0) J_x(t) \rangle dt = \frac{V}{3k_B T^2} \int_0^\infty \langle J(0) \cdot J(t) \rangle dt \quad (\text{a-8})$$

In the x-direction, $J_x(0)$ and $J_x(t)$ show the heat HF currents at every time and the simulation's initial moment. On the other hand, the sentence inside the integral referred to the average HF function. The HF vector was obtained from the following equation:

$$\begin{aligned} J &= \frac{1}{V} \left[\sum_i \mathbf{e}_i v_i - \sum_i S_i v_i \right] \\ &= \frac{1}{V} \left[\sum_i \mathbf{e}_i v_i - \sum_{i < j} \left(f_{ij} v_j \right) x_{ij} \right] \\ &= \frac{1}{V} \left[\sum_i \mathbf{e}_i v_i - \frac{1}{2} \sum_{i < j} \left(f_{ij} \cdot \left(v_i + v_j \right) x_{ij} \right) \right] \end{aligned} \quad (\text{a-9})$$

Data availability

No data was used for the research described in the article.

References

- [1] S. Ali, M. A. B. R.A. Hussein, S. Babadoust, N.S.S. Singh, S. Salahshour, S. Baghaei, Numerical study of thermal performance of silica-aerogel/paraffin nanostructure in the presence of CuO nanoparticles: a molecular dynamics approach, *Nano-Struct. Nano-Objects* 41 (101435) (2025) 101435, <https://doi.org/10.1016/j.nano.2025.101435>.
- [2] J. Yang, A.B.M. Ali, Y.M.A. Al-zahy, N.S. Sawaran Singh, M. Al-Bahrani, T. Orlova, S. Esmaeili, The effect of copper oxide nanoparticles on the thermal behavior of silica aerogel/paraffin as a phase change material in a cylindrical channel with molecular dynamics simulation, *Prog. Nucl. Energy* 181 (105645) (2025) 105645, <https://doi.org/10.1016/j.pnucene.2025.105645>.
- [3] Y. Liu, A. Basem, Y.M.A. Al-zahy, N.S.S. Singh, M. Al-Bahrani, D. Abduvalieva, S. Esmaeili, Molecular dynamics simulation of thermal behavior of paraffin/Cu nanoparticle PCM in a non-connected rotating ribbed tube, *Int. Commun. Heat. Mass Transf.* 165 (109058) (2025) 109058, <https://doi.org/10.1016/j.icheatmasstransfer.2025.109058>.
- [4] Q. An, M. Bagheritabar, A. Basem, A.A. Ghabra, Y. Li, M. Tang, R. Sabetvand, The effect of size of copper oxide nanoparticles on the thermal behavior of silica aerogel/paraffin nanostructure in a duct using molecular dynamics simulation, *Case Stud. Therm. Eng.* 60 (104666) (2024) 104666, <https://doi.org/10.1016/j.csite.2024.104666>.
- [5] Y. Huang, S.S. Kamoona, M. Kaur, A. Basem, M.H. Khaddour, M. Al-Bahrani, N. Emami, The effect of initial pressure and atomic concentration of iron nanoparticles on thermal behavior of sodium sulfate/magnesium chloride hexahydrate nanostructure by molecular dynamics simulation, *Therm. Sci. Eng. Prog.* 53 (102697) (2024) 102697, <https://doi.org/10.1016/j.tsep.2024.102697>.
- [6] M.K. Pasupathi, K. Alagar, M.J. S. P, M. MM, G. Aritra, Characterization of hybrid-nano/paraffin organic phase change material for thermal energy storage applications in solar thermal systems, *Energies* 13 (19) (2020) 5079.
- [7] N. Aslfattahi, R. Saidur, A. Arifuzzaman, R. Sadri, N. Bimbo, M.F.M. Sabri, P. A. Maughan, L. Bouscarrat, R.J. Dawson, S.M. Said, Experimental investigation of energy storage properties and thermal conductivity of a novel organic phase change material/MXene as A new class of nanocomposites, *J. Energy Storage* 27 (2020) 101115.
- [8] C. Xu, W. Wang, H. Zhang, G. Fang, Polyethylene glycol/polyvinyl butyral/graphene nanoplates as composite phase-change materials with high thermal conductivity, *Sol. Energy Mater. Sol. Cells* 250 (2023) 112093.
- [9] Y. Chen, W. Wang, G. Fang, Thermal performance of lauric acid/bentonite/carbon nanofiber composite phase-change materials for heat storage, *J. Mater. Eng. Perform.* 33 (1) (2024) 348–361.
- [10] C. Zhao, C. Yang, Y. Tao, Y. He, Interfacial nanolayer effect on thermophysical properties of silica-paraffin phase change material-A molecular dynamics simulation, *Int. J. Heat. Mass Transf.* 220 (2024) 125007.
- [11] A.S.M. Aljaloud, K. Smida, H.F.M. Ameen, M. Albedah, I. Tlili, Investigation of phase change and heat transfer in water/copper oxide nanofluid enclosed in a cylindrical tank with porous medium: a molecular dynamics approach, *Eng. Anal. Bound. Elem.* 146 (2023) 284–291.

- [12] J. Fereidooni, Heat transfer inspection of nano-encapsulated phase change materials inside a Γ -shaped enclosure influenced by magnetic field, *J. Magn. Magn. Mater.* 561 (2022) 169682.
- [13] L. Ze, F. Al-dolaimy, S.M. Sajadi, M.T. Qasim, A.H. Alawadi, R.B. Dehkordi, A. Alsalamy, R. Sabetvand, M. Hekmatifar, The effect of number of nanoparticles on atomic behavior and aggregation of CuO/water nanofluid flow in microchannels using molecular dynamics simulation, *Eng. Sci. Technol., Int. J.* 47 (2023) 101556.
- [14] G. Yan, O.S. Mahdy, A. Alizadeh, N. Nasajpour-Esfahani, S. Esmaeili, M. Hekmatifar, M.R. El-Sharkawy, A.S. Al-Shat, M. Shamsborhan, Effects of initial temperature, initial pressure, and external heat flux on the thermal behavior of ethanol/biodiesel as biomass structures, *Case Stud. Therm. Eng.* 50 (2023) 103399.
- [15] M.B. Henda, T.A. Alkanhal, A. Rebey, A. Sa'ed, I. Tlili, High-efficiency perovskite photovoltaic system performance by molecular dynamics method: optimizing electron transport thicknesses, hole transport, and anti-reflector layers of the sustainable energy materials, *Eng. Anal. Bound. Elem.* 150 (2023) 120–126.
- [16] Q.H. Le, Z. Hussain, N. Khan, S. Zuev, K. Javid, S.U. Khan, Z. Abdelmalek, I. Tlili, Chebyshev collocation simulations for instability of Hartmann flow due to porous medium: a neutral stability and growth rate assessment, *Ain Shams Eng. J.* 14 (12) (2023) 102215.
- [17] S.M. AlDosari, S. Banawas, H.S. Ghafour, I. Tlili, Q.H. Le, Drug release using nanoparticles in the cancer cells on 2-D materials in order to target drug delivery: a numerical simulation via molecular dynamics method, *Eng. Anal. Bound. Elem.* 148 (2023) 34–40.
- [18] A.S.M. Aljaloud, L. Manai, I. Tlili, Bioconvection flow of Cross nanofluid due to cylinder with activation energy and second order slip features, *Case Stud. Therm. Eng.* 42 (2023) 102767.
- [19] S. Banawas, T.K. Ibrahim, I. Tlili, Q.H. Le, Reinforced calcium phosphate cements with zinc by changes in initial properties: a molecular dynamics simulation, *Eng. Anal. Bound. Elem.* 147 (2023) 11–21.
- [20] H. Tafirishi, S. Sadeghzadeh, R. Ahmadi, Molecular dynamics simulations of phase change materials for thermal energy storage: a review, *RSC Adv.* 12 (23) (2022) 14776–14807.
- [21] H. Tafirishi, S. Sadeghzadeh, R. Ahmadi, F. Molaei, F. Yousefi, H. Hassanloo, Investigation of tetracosane thermal transport in presence of graphene and carbon nanotube fillers—a molecular dynamics study, *J. Energy Storage* 29 (2020) 101321.
- [22] H. Hassanloo, S. Sadeghzadeh, R. Ahmadi, Reactive molecular dynamics simulation of thermo-physicochemical properties of non-covalent functionalized graphene nanofluids, *Mater. Today Commun.* 32 (2022) 103869.
- [23] H. Hassanloo, S. Sadeghzadeh, R. Ahmadi, A new approach to dispersing and stabilizing graphene in aqueous nanofluids of enhanced efficiency of energy-systems, *Sci. Rep.* 10 (1) (2020) 7707.
- [24] S. Giannakis, I. Hendaoui, M. Jovic, D. Grandjean, L.F. De Alencastro, H. Girault, C. Pulgarin, Solar photo-Fenton and UV/H₂O₂ processes against the antidepressant Venlafaxine in urban wastewaters and human urine. Intermediates formation and biodegradability assessment, *Chem. Eng. J.* 308 (2017) 492–504.
- [25] Y. Yu, Y. Tao, Y.-L. He, Molecular dynamics simulation of thermophysical properties of NaCl-SiO₂ based molten salt composite phase change materials, *Appl. Therm. Eng.* 166 (2020) 114628.
- [26] L. Quan, Z. Pan, Investigating the thermal behavior of phase change materials of ethylene glycol-filled SiO₂ plates in the presence of solar radiation by molecular dynamics simulation, *Eng. Anal. Bound. Elem.* 150 (2023) 1–6.
- [27] S.K. Singh, S.K. Verma, R. Kumar, Thermal performance and behavior analysis of SiO₂, Al₂O₃ and MgO based nano-enhanced phase-changing materials, latent heat thermal energy storage system, *J. Energy Storage* 48 (2022) 103977.
- [28] C. Zhao, Y. Tao, Y. Yu, Molecular dynamics simulation of thermal and phonon transport characteristics of nanocomposite phase change material, *J. Mol. Liq.* 329 (2021) 115448.
- [29] M.D. Hanwell, D.E. Curtis, D.C. Lonie, T. Vandermeersch, E. Zurek, G.R. Hutchison, Avogadro: an advanced semantic chemical editor, visualization, and analysis platform, *J. Cheminform.* 4 (2012) 1–17.
- [30] L. Martínez, R. Andrade, E.G. Birgin, J.M. Martínez, PACKMOL: a package for building initial configurations for molecular dynamics simulations, *J. Comput. Chem.* 30 (13) (2009) 2157–2164.
- [31] A.S. Aldossary, N. Sulaiman, PCM examine of Silica/Decane nanostructure in the presence of copper oxide nanoparticles to improve the solar energy capacity of glass in the solar collectors via MD approach, *Eng. Anal. Bound. Elem.* 145 (2022) 72–82.
- [32] X. Liu, M. Adibi, M. Shahgholi, I. Tlili, S.M. Sajadi, A. Abdollahi, Z. Li, A. Karimipour, Phase change process in a porous Carbon-Paraffin matrix with different volume fractions of copper oxide Nanoparticles: a molecular dynamics study, *J. Mol. Liq.* 366 (2022) 120296.
- [33] L. Verlet, Computer "experiments" on classical fluids. I. Thermodynamical properties of Lennard-Jones molecules, *Phys. Rev.* 159 (1) (1967) 98.
- [34] W. Press, S. Teukolsky, W. Vetterling, B. Flannery, Section 16.2. Viterbi Decoding, *Numer. Recipe.: Art. Sci. Comput.* (2007).
- [35] A. Oluwajobi, X. Chen, The effect of interatomic potentials on the molecular dynamics simulation of nanometric machining, *Int. J. Autom. Comput.* 8 (2011) 326–332.
- [36] N. Von Solms, R. O'lenick, Y. Chiew, Leonard-Jones chain mixtures: variational theory and Monte Carlo simulation results, *Mol. Phys.* 96 (1) (1999) 15–29.
- [37] H.J. Berendsen, J.R. Grigera, T.P. Straatsma, The missing term in effective pair potentials, *J. Phys. Chem.* 91 (24) (1987) 6269–6271.
- [38] A.K. Rappé, C.J. Casewit, K. Colwell, W.A. Goddard III, W.M. Skiff, UFF, a full periodic table force field for molecular mechanics and molecular dynamics simulations, *J. Am. Chem. Soc.* 114 (25) (1992) 10024–10035.
- [39] S.L. Mayo, B.D. Olafson, W.A. Goddard, DREIDING: a generic force field for molecular simulations, *J. Phys. Chem.* 94 (26) (1990) 8897–8909.
- [40] M.S. Green, Markoff random processes and the statistical mechanics of time-dependent phenomena. II. Irreversible processes in fluids, *J. Chem. Phys.* 22 (3) (1954) 398–413.